Supplementary Material

1 Model configurations

The model configurations and inputs are presented in Table S1. The anthropogenic emission inventory is from the Multi-resolution Emission Inventory for China (MEIC) [1] for the base year 2010. The Model of Emissions of Gases and Aerosols from Nature (MEGAN) version 2 [2] is applied for online calculation of the biogenic emissions. Dust emissions are online calculated as well using the option of Model for Simulating Aerosol Interactions and Chemistry (MOSAIC) and the Modal Aerosol Dynamics Model for Europe (MADE)/Seconday Organic Aerosol Model (SORGAM) [3]. The sea-salt emissions are calculated using the method by Gong [4-6].

Table S1. Model configurations in this study.

Physical and chemical presses	Configuration
Simulation period	January 1-31, 2013
Domain	East Asia (36-km), northern China (12-km)
Horizontal resolution	36-km and12-km
Vertical resolution	23 layers from 1000-100 mb
Anthropogenic emissions	MEIC [http://www.meicmodel.org/][1]
Biogenic emissions	MEGAN 2 [2]
Dust emissions	MOSAIC and MADE/SORGAM dust emissions [3]
Sea-salt emissions	Gong et al. [4-6]
Meteorological ICs and BCs	The National Centers for Environmental Prediction Final Analysis (NCEP-FNL) reanalysis data
Chemical IC and BC	Default for 36-km; nested down from the parent domain for 12-km
Gas-phase chemistry	CBMZ [7]
Photolysis	Madronich F-TUV [9]
Aerosol module	8-bin MOSAIC aerosol module [8]
Urban surface	Urban canopy model [10]
Shortwave radiation	Goddard [11]
Longwave radiation	RRTM [12]
Land surface	NOAH Land Surface Model [13]
Surface layer	Monin-Obukhov [14]
PBL	Yonsei University Scheme (YSU) [15]
Cumulus	Grell 3D ensemble [16]
Microphysics	Purdue Lin [17];
aer_ra_feedback	1 (on) and 0 (off) for baseline and sensitivity simulation

The Carbon-Bond Mechanism version Z (CBMZ) [7] is chosen as the gas-phase chemical chemistry. The MOSAIC that uses 8 volatility bins is used as aerosol module [8]. The Madronich Fast Troposphere Ultraviolet Visible (F-TUV) photolysis scheme [9] and the urban canopy model [10] are applied for photolytic rate calculation and urban surface scheme, respectively.

Other physical modules are: Goddard shortwave and RRTM long wave radiation schemes [11,12], the Noah land surface model [13], the Monin-Obukhov surface layer model [14], the Yonsei University (YSU) PBL scheme [15], the Grell 3D ensemble cumulus parameterization [16], and the Purdue Lin microphysics scheme [17]. Those physics options have been applied extensively in past studies [18-22].

2 Evaluation of model performance

2.1 Meteorological predictions

The overall statistics of the model performance on meterological predictions, including T2, Q2, WS10, WD10, and precipitation are summarized in Table S2. To comparing the impact of aerosol-meteorology feedbacks on those meteorological parameters, the statistics of the BASE and the NF simulations are both presented in Table S2. Generally, T2 is underpredicted by the model, with the MBs of -1.4 ℃ (-1.4 K) over Domain 1 at 36 km resolution, and -1.4℃ and -0.8 ℃ over Domain 2 at 36 and 12 km resolutions, respectively, in the BASE simulation. Those numbers are over the criteria (MB ≤ for a satisfactory performance proposed by Emery et al. [23] and Tesche et al. [24], partially due to not involving the Four-Dimentional Data Assimilation (FDDA) technique in this simulation to correctly quantify the aerosol feedbacks. But those results are generally better than the performance of the optimized configuration set for WRF/Chem over the North China in Wang et al. [19] (MBs of -1.2 ℃ over Domain 1 at 36 km, and -1.7℃ and -1.2 ℃ over Domain 2 at 36 and 12 km, respectively, with slightly different physical configurations and FDDA), and also better than the performance of the Mesoscale Modeling System Generation 5 and the Models-3/Community Multiscale Air Quality Model (MM5-CMAQ) system in Wang et al. [25] (MBs of -1.5 ℃

over Domain 1 at 36 km, and -1.2℃ and -1.1 ℃ over Domain 2 at 36 and 12 km, respectively) over the same domains for same period, especially over Domain 2 at fine grid resolution. When turning off the radiative feedbacks of aerosol (NF simulation), the predicted T2 will be increased 0.2 ℃ on average over both Domain 1 (-3.4 ℃ to -3.2 ℃) and Domain 2 (-4.4 ℃ to -4.2 ℃) because of the lack of calculating radiation scattering and absorption of atmospheric aerosols in NF simulation, which will cool the atmosphere.

Table S2. Overall statistics of meteorological predictions over Domain 1 at 36 km resolution and Domain 2 at 36 and 12 km resolution in baseline (BASE) and no-feedback (NF) simulations.

Variable	Simulation name	Domain	Grid size /(km)	Obs.	Sim.	MB	RMSE /(%)	NMB /(%)	NME /(%)
T2 (℃)	BASE	1	36	-2.0	-3.4	-1.4	4.7	-71	-178
	BASE	2	36	-3.6	-5.0	-1.4	4.2	-38	-88
	BASE	2	12	-3.6	-4.4	-0.8	3.9	-22	-82
	NF	1	36	-2.0	-3.2	-1.2	4.7	-59	-177
	NF	2	36	-3.6	-4.7	-1.1	4.2	-29	-88
	NF	2	12	-3.6	-4.2	-0.6	3.9	-16	-81
Q2 ($kg \cdot kg^{-1}$)	BASE	1	36	0.0026	0.0028	0.0002	0.0010	7	25
	BASE	2	36	0.0021	0.0022	0.0001	0.0006	4	20
	BASE	2	12	0.0021	0.0022	0.0001	0.0006	5	20
	NF	1	36	0.0026	0.0028	0.0002	0.0010	8	25
	NF	2	36	0.0021	0.0022	0.0001	0.0006	5	21
	NF	2	12	0.0021	0.0022	0.0001	0.0006	6	20
WS10 ($m \cdot s^{-1}$)	BASE	1	36	2.0	4.2	2.20	3.23	112	131
	BASE	2	36	2.2	4.1	1.88	2.88	86	105
	BASE	2	12	2.2	4.0	1.80	2.86	82	103
	NF	1	36	2.0	4.2	2.23	3.25	114	132
	NF	2	36	2.2	4.1	1.90	2.90	87	106
	NF	2	12	2.2	4.0	1.81	2.87	83	104
WD10 (^{o})	BASE	1	36	196.2	183.4	7.3	79.0	4	31
	BASE	2	36	199.3	218.0	3.4	73.0	2	28
	BASE	2	12	199.3	195.6	0.9	73.0	0	28
	NF	1	36	196.2	182.8	7.7	79.1	4	31
	NF	2	36	199.3	217.4	3.9	73.1	2	28
	NF	2	12	199.3	194.5	1.2	72.9	1	28
Precipitation (mm)	BASE	1	36	1.3	1.3	-0.1	3.2	-4	111
	BASE	2	36	2.2	2.1	0.0	3.5	0	86
	BASE	2	12	2.2	1.7	-0.4	5.6	-19	105
	NF	1	36	1.3	1.3	-0.1	3.2	-4	111
	NF	2	36	2.2	2.1	0.0	3.5	0	86
	NF	2	12	2.2	1.7	-0.5	5.2	-22	106

Water vapor mixing ratio is well predicted by the model, with the MBs of 0.0002 $kg \cdot kg^{-1}$ over Domain 1 at 36 km resolution, and 0.0001 $kg \cdot kg^{-1}$ over Domain 2 at both 36 and 12 km resolutions, which are all within the criteria of MB ≤ 1$g \cdot kg^{-1}$ for Q2. The statistics of the NF simulation do not show notable differences comparing to the BASE, indicating that turning off the aerosol-meteorology feedbacks will not result in obvious differences in Q2 predictions, which is consistent to the results of Wang et al. [26].

As for wind speed, the model overall overpredict the WS10, with MBs of 2.2 $m \cdot s^{-1}$ over Domain 1, and 1.9 and 1.8 $m \cdot s^{-1}$ over Domain 2 at 36 and 12 km resolutions, respectively, which are over the guidance of Emery et al. [23] and Tesche et al. [24] (MB ≤ 1$m \cdot s^{-1}$), and also larger than the statistics in Wang et al. [19] using WRF/Chem (0.7 $m \cdot s^{-1}$ over Domain 1, and 0.1 $m \cdot s^{-1}$ over Domain 2 at both resolutions), but better the predictions in Zhang et al. [27] (2.0 $m \cdot s^{-1}$ over eastern China at 27 km grid resolution). Note one big difference between this study and Wang et al. [19] is that the FDDA is not applied in the simulations in this study, because the data assimilation press will overcome the

signals introduced by radiative effects of atmospheric aerosols. This is one of the reasons for the large bias of WS10. This overpredictions will result in underpredictions of air pollutants concentrations. Comparing to the NF simulation, it can be seen that wind speed will be sightly decrease when considering the aerosol-meteorological feedbacks, e.g., 0.07 $m \cdot s^{-1}$ on average over Domain 2, which is also consistent with Wang et al. [19], that the aerosol feedbacks will slow the wind speed and lead to more stable atmosphere. Wind direction is well reproduced with MBs of 7.3° over Domain 1, and 3.4° and 0.9° over Domain 2 at 36 and 12 km resolutions, respectively, which are larger than the statistics in Wang et al. [19] (MBs of 4.0 degree over Domain 1, and -0.3 and -0.7 degree over Domain 2 at 36 and 12 km resolutions, respectively), but still within the criteria of MB ≤ 1 for WD10. The statistics for WD10 in NF are slightly worse than in BASE, as shown in Table S2, indicating that the ignoring the aerosol radiative feedbacks will worsen the model performance on WD10.

Daily precipiations are well predicted with MBs of -0.1 mm over Domain 1, and 0.0 and -0.4 mm over Domain at 36 and 12 km resolutions, respectively, which are close to the MBs in Wang et al. [19] of 0.0 mm over Domain 1 and -0.4 mm over Domain 2 at both resolutions. The results of NF and BASE are quite similar because the indirect effects of aerosol to meteorology, e.g., cloud formation, precipation, are not studied in the simulations in this study.

In general, the model predictions on general meteorological variables are acceptable, except for the overestimation of wind speed at 10 m, which seems to be a common issue for the WRF/Chem model [28]. Further evaluation and discussion on downward shortwave flux at the surface (SWDOWN) and planetary boundary layer (PBL) height will be dicussed in Section 3 below.

2.2 Air quality predictions

The overall statistics for air quality predictions over Domain 1 at 36 km resolution and Domain 2 at both 36 and 12 km resolutions are summarized in Table S3, including the pollutants of $PM_{2.5}$, PM_{10}, SO_2, and NO_2. The statistics for the NF simulation are included as well as a comparison to the BASE. The model under predict the $PM_{2.5}$ concentrations in general, with the NMBs of -33% over Domain 1 at 36 km, and -27% and -23% over Domain 2 at 36 and 12 km resolutions, respectively, which are comparable to the NMBs of -24%, -16%, -3%, and -19% for Shijiazhuang, Jinan (the capital of Shandong Province), Beijing, and Tianjin in Wang et al. [26], and -18.9% for eastern China in Zhang et al. [27]. This underprediction can be partially attributed to the overestimation of the wind speed, as discussed in the above section 2.1. In the WRF/Chem simulations of Wang et al. [19] over the same domain for the same period, the $PM_{2.5}$ concentrations are overall overpredicted by 31% over Domain 1 and 70% over Domain 2 due to the lack of wet scavenging in those simulations (the differences in the model configuration in Wang et al. [19] comparing to this study are: SAPRC99 [29,30] is chosen as the gas phase mechanism instead of CBMZ [7] in this study; 4 bin MOSAIC aerosol module with volatility basis set (VBS) [8,31] is used instead of 8 bin MOSAIC module [8]; Kain-Fritsch cumulus scheme [32] is applied instead of Grell 3D ensemble [33]; GOCART online dust emission module [34] is chosen instead of MOSAIC and MADE/SORGAM dust emissions [3]; and FDDA is applied. The SAPRC99 module is not fully coupled with the scheme of wet scavenging). The MFBs and MFEs are -40% and 66% over Domain 1 at 36 km, and -33% and 67% over Domain 2 at 12 km, respectively, which are all within the criteria of MFB ≤ 60% and MFE ≤ 75% [35]. After turning off the aerosols radiative feedbacks, the predicted concentrations of $PM_{2.5}$ are slightly decreased (2.5 $\mu g \cdot m^{-3}$ over Domain 1 and 1.8 $\mu g \cdot m^{-3}$ over Domain 2), with the overall NMBs of -35% (vs. -33%) over Domain 1 at 36 km, and -28% (vs. -27%) and -25% (vs. -23%) over Domain 2 at 36 and 12 km resolutions. It is understandable that the extinction of atmospheric aerosols will cause a decrease in solar radiation on the surface, which lead to a decrease in surface temperature, and at the same time, the light absorption of the upper layer particles will strengthen the temperature inversion in the upper PBL. Both effects lead to a decrease in PBL height and thus an increase in pollutants concentrations.

The PM_{10} concentrations are underpredicted as well partially due to the overprediction of wind speed, with the NMBs of -48% over Domain 1 at 36 km resolution, and -45% and -43% over Domain 2 at 36 and 12 km resolutions, respectively. The larger negative biases in PM_{10} comparing to $PM_{2.5}$ indicate that the model underestimates the concentrations in $PM_{2.5-10}$, which is consistent to the predictions in Wang et al. [19]. Nevertheless, the MFBs and MFEs are -59% and 73% over Domain 1 at 36 km resolution, and -56% and 75% over Domain 2 at 12 km resolution, respectively, which still meet the criteria. In the NF simulation, the negative biases are larger than those for the BASE by 1–4%. Comparison to the BASE, the aerosol feedbacks will lead to an increase in PM_{10} concentrations at 2.3 $\mu g \cdot m^{-3}$ and 2.2 $\mu g \cdot m^{-3}$ for Domain 1 and 2, respectively.

The major species in $PM_{2.5}$, i.e., sulfate, nitrate, ammonia and EC are also evaluated to assess the model performance on $PM_{2.5}$ chemical compositions. The observation data available to this study includes the observations at a site located in the Hebei University of Engineering (refer to as HEBEU) in Handan by the leading author's group of this paper [36], and the data from the site in Tsinghua University (THU) published in Wang et al. [37]. Fig. S1 shows the comparison of the observed and predicted (by BASE and NF) daily average concentrations of major $PM_{2.5}$ chemical constituents. It can be seen that at THU site in Beijing, our predictions are quite similar to those in Wang et al. [37], that all the $PM_{2.5}$ species are significantly underestimated, especially for sulfate, nitrate, and ammonia. Those can be mostly attributed by the ignorance of the heterogeneous chemistry occurred in the atmosphere but not involved in the present model [37, 38]. At the HEBEU site in Handan, the $PM_{2.5}$ concentrations are overall overpredicted,

especially for OC and EC, but the concentrations of sulfate, nitrate, and ammonia are still underestimated. When considering the aerosol-meteorological feedbacks, the concentrations of OC and EC will increase mainly due to the lower PBL, but nitrate and ammonia concentrations will slightly decrease.

SO_2 concentrations are overall slightly underpredicted over Domain 1 (NMB of -9%) and Domain 2 (NMB of -6%) at 36 km grid resolution, and overpredicted (NMB of 41%) over Domain 2 at 12 km resolution, which is consistent to the SO_2 predictions in Wang et al. [19]. This alternation of biases can be mainly attributed to the uncertainties in the spatial allocation of the emissions into fine grid in the emission inventory, which has been extensively discussed in Wang et al. [25] and Wang et al. [19]. Comparing to the NF case, the predicted SO_2 concentrations in BASE are 4.0–7.5 $\mu g \cdot m^{-3}$ (5–8%) higher than in NF.

NO_2 concentrations are well predicted with NMBs of -18% over Domain 1 at 36km resolution, and 36% and 10% over Domain 2 at 36 and 12 km resolutions, respectively. The predicted NO_2 concentrations in BASE are 0.8–1.5 $\mu g \cdot m^{-3}$ (1–3%) higher than the predictions in NF. The overall model performance on SO_2 and NO_2 predictions are better than in Wang et al. [19].

In summary, although the WRF/Chem model tends to under predict the concentrations of $PM_{2.5}$ and PM_{10}, which may partially due to the overprediction of wind speed, it still produces an acceptable prediction to be used in further analysis. Considering aerosol direct feedbacks will lead to an average increase of 1.8 $\mu g \cdot m^{-3}$ (~2%) in $PM_{2.5}$, 2.2 $\mu g \cdot m^{-3}$ (~2%) in PM_{10}, 7.5 $\mu g \cdot m^{-3}$ (~6%) in SO_2, and 0.8 $\mu g \cdot m^{-3}$ (~1%) in NO_2 concentrations over Domain 2 at 12 km grid resolution.

Table S3. Overall statistics of $PM_{2.5}$, PM_{10}, SO_2, and NO_2 predictions over Domain 1 at 36 km resolution and Domain 2 at 36 and 12 km resolution in baseline (BASE) and no-feedback (NF) simulations.

Pollutants	Simulation name	Domain	Grid size (km)	Obs.	Sim.	MB	NMB (%)	NME (%)	MFB (%)	MFE (%)
$PM_{2.5}$ ($\mu g \cdot m^{-3}$)	BASE	1	36	137.2	91.9	-45.3	-33	54	-40	66
	BASE	2	36	155.3	113.9	-41.4	-27	50	-27	58
	BASE	2	12	155.3	118.9	-36.5	-23	57	-33	67
	NF	1	36	137.2	89.4	-47.8	-35	54	-41	67
	NF	2	36	155.3	111.7	-43.6	-28	51	-28	59
	NF	2	12	155.3	117.1	-38.2	-25	56	-33	66
PM_{10} ($\mu g \cdot m^{-3}$)	BASE	1	36	195.0	102.4	-92.7	-48	57	-59	73
	BASE	2	36	222.1	122.5	-99.7	-45	55	-51	67
	BASE	2	12	222.1	126.5	-95.6	-43	57	-56	75
	NF	1	36	195.0	100.1	-94.9	-49	58	-60	74
	NF	2	36	222.1	120.5	-101.6	-46	55	-52	69
	NF	2	12	222.1	124.3	-97.8	-44	57	-57	75
SO_2 ($\mu g \cdot m^{-3}$)	BASE	1	36	74.8	68.4	-6.4	-9	83	-33	86
	BASE	2	36	99.2	93.5	-5.7	-6	75	-10	75
	BASE	2	12	99.2	139.7	40.5	41	113	-4	87
	NF	1	36	74.8	64.5	-10.3	-14	82	-37	87
	NF	2	36	99.2	88.4	-10.8	-11	75	-14	76
	NF	2	12	99.2	132.2	32.9	33	109	-7	86
NO_2 ($\mu g \cdot m^{-3}$)	BASE	1	36	63.5	52.2	-11.3	-18	48	-27	62
	BASE	2	36	65.6	68.6	3.0	5	43	8	48
	BASE	2	12	65.6	71.9	6.3	10	51	2	56
	NF	1	36	63.5	50.7	-12.8	-20	49	-32	66
	NF	2	36	65.6	67.8	2.2	3	44	5	49
	NF	2	12	65.6	71.1	5.5	8	51	0	56

3 Aerosol direct effects on meteorology

3.1 Surface solar radiation

To further evaluate the model performance on radiation predictions, as well as assess the aerosol direct effects on radiation, we used the satellite observation data from the Clouds and Earth's Radiant Energy System (CERES) on solar radiation, i.e., the SWDOWN, due to the lack of surface observations in China. This dataset provides both solar-reflected and Earth-emitted radiation from the top of the atmosphere to the Earth's surface, computed from the observations from several satellite instruments such as the Moderate Resolution Imaging Spectroradiometer (MODIS). The detailed description can be found at http://ceres.larc.nasa.gov/index.php.

Figure S2 presents the comparison of the observed and predicted SWDOWN, by both the BASE and NF simulations, over Domain 1 and 2 at 36 and 12 km resolution, respectively, as well as the differences between the BASE and NF. The original CERES datasets are of $1^o \times 1^o$ resolution and were linearly interpolated into 36 and 12 km grid resolution. Table S4 summarizes the overall statistics for the two simulations. The model generally capture the spatial distributions of SWDOWN over Domain 1 and 2 (first two column of Fig. S2a, b), with over predictions mainly appear in the Tibet region, the south of the Yangtze River, and northern China (see Fig. S2a for Domain 1). Over Domain 2 the overpredictions are more obvious with the overall NMB of 33% and 46% for BASE and NF, respectively (note in Fig. S2b the legend scales of the CERES data and the predictions are different). However, it still can be seen that if not considering the aerosol radiative feedbacks, the spatial distributions of SWDOWN will be quite different from the observations (the NF case in Fig. S2b). Although SWDOWN is overall overpredicted in the BASE case, it still captures the spatial distribution, especially the lower SWDOWN band from the intersection of Henan and Shandong, upward to southern Hebei, Tianjin, through Bohai Bay to Liaoning Province. The overall statistics of the MB, NMB and correlation coefficient (Corr. Coeff.) are 20.4 $W \cdot m^{-2}$, 17%, and 0.86, respectively, for Domain 1, and 33.9 $W \cdot m^{-2}$, 33%, and 0.37, respectively, for Domain 2. Note the relatively small Corr. Coeff. for Domain 2 can be partially attributed to the interpolation of the CERES observations of $1^o \times 1^o$ to the fine resolutions (36 and 12 km).

Table S4. Overall statistics of monthly-average downward shortwave radiation flux at surface (SWDOWN) of the BASE and NF over Domain 1 and 2.

Simulation name	Domain	CERES ($W \cdot m^{-2}$)	Sim. ($W \cdot m^{-2}$)	MB ($W \cdot m^{-2}$)	RMSE ($W \cdot m^{-2}$)	NMB (%)	NME (%)	Corr. Coeff.
BASE	1	120.0	141.5	20.4	28.0	17	19	0.86
NF	1		150.5	29.4	37.4	24	26	0.81
BASE	2	101.6	135.5	33.9	36.9	33	33	0.37
NF	2		148.6	47.0	50.3	46	46	0.08

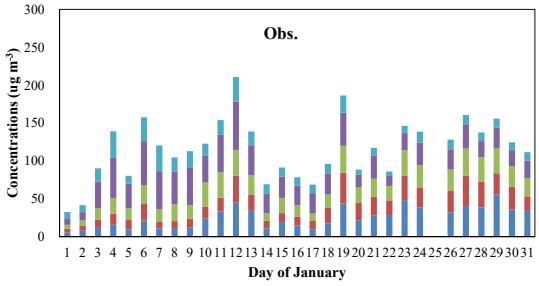

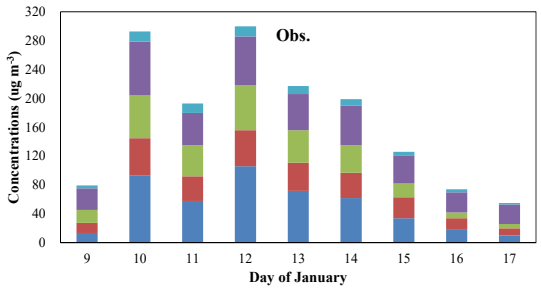

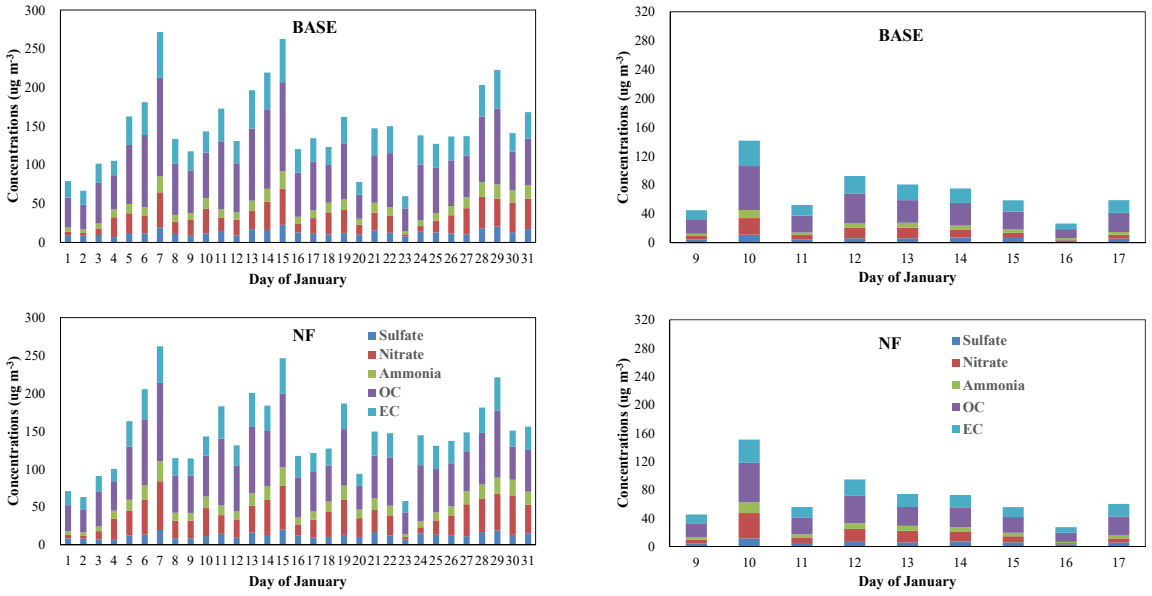

Fig. S1. Comparison of observed and predicted (by BASE and NF) daily average concentrations of $PM_{2.5}$ chemical constituents at HEBEU site in Handan (a) and at THU site in Beijing (b).

The discrepancies between the BASE and NF simulations depict the aerosol direct effects on solar radiation. In Domain 1, the largest decrease in SWDOWN occurs over the central eastern China, including southern Hebei, Henan, Hubei, and northern Hunan, and the Sichuan Basin, at about 20–50 $W \cdot m^{-2}$ (15–35%) of the BASE simulation. It is understandable that this spatial distribution is similar to the distribution of $PM_{2.5}$ concentrations (see Fig. 2a). In Domain 2, the largest discrepancy appears over the line from southern Beijing, through southern Hebei to the middle of Henan Province, where has the highest $PM_{2.5}$ concentrations (see Fig. 2a). Over the southern Hebei cities this paper concerns, the decreases induced by aerosol direct feedbacks are 20–34 $W \cdot m^{-2}$ (16–30%). In Wang et al. [26], the predicted reduction in SWDOWN over Beijing and Tianjin are 26% and 31%, respectively, by the WRF-CMAQ model. Our results are consistent with theirs.

Surface observations on solar radiation available to this study are only the data used in Wang et al. [26] for Beijing and Tianjin from China Meteorological Data Sharing Service System (http://cdc.cma.gov.cn/). The comparison of the observed and simulated daily surface solar radiations, by the both simulations of BASE and NF, is shown in Fig. S3. It can be seen that the NF simulation cannot capture the temporal variations of the radiation in Beijing, especially the large and rapid decrease during January 11–15 (Fig. S3a), which turns out to be the most polluted period in that month. The $PM_{2.5}$ concentrations reached as high as more than 300 $\mu g\ m^{-3}$ on daily average [25]. When considering the aerosol feedbacks, the overprediction of radiation is reduced and the temporal variations are better reproduced. The NMBs are reduced from 84% in NF to 52% in BASE for Beijing. The Tianjin's case is similar that the NMBs are reduced from as high as 115% in NF to 75% in BASE, although this bias is higher than that in Wang et al. [26]. Nevertheless, neglecting the aerosol direct effects will result in larger positive biases (around 20% in Beijing and Tianjin) in surface radiation predictions, especially for the areas and periods which have higher $PM_{2.5}$ loadings, which are exactly the place and time of the most concerns.

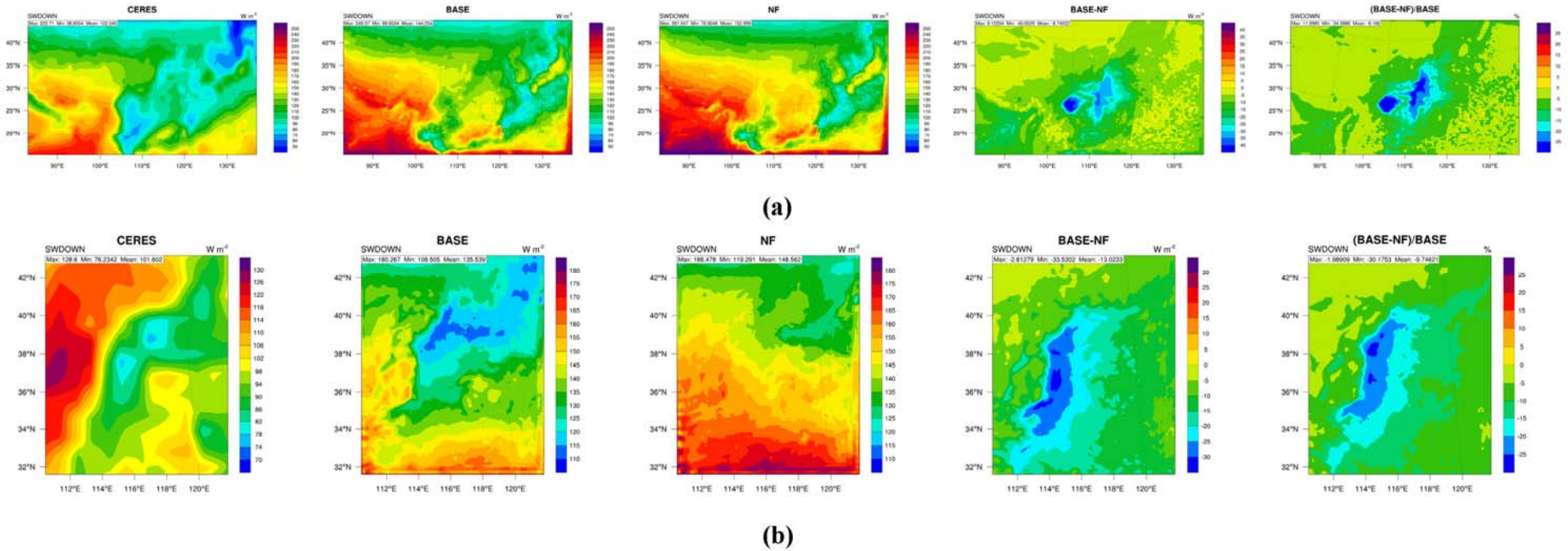

Fig. S2. Monthly-average downward shortwave radiation flux at surface (SWDOWN) from the observations of CERES, and the predictions from BASE and NF, and their differences in absolute value (BASE-NF) and percentage ((BASE-NF)/BASE) over Domain 1 (a) and Domain 2 (b).

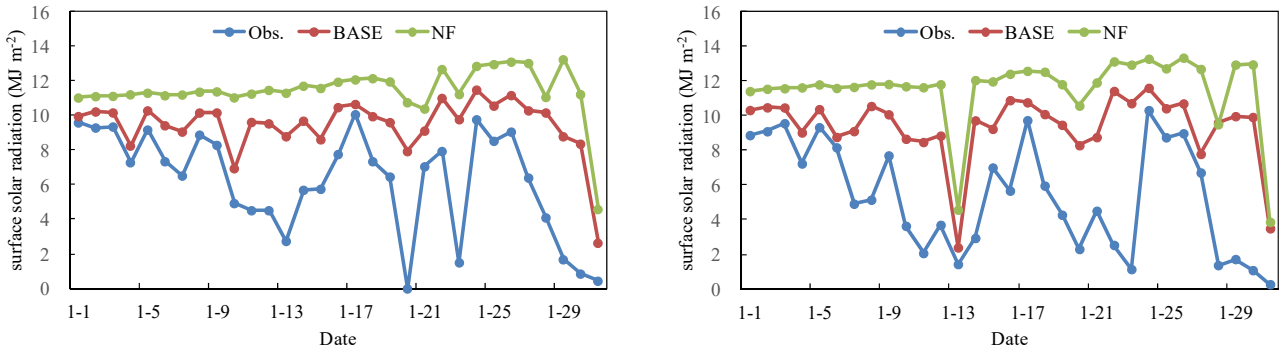

(a) Beijing (NMB_{BASE} = 52%, NMB_{NF} = 84%) (b) Tianjin (NMB_{BASE} = 75%, NMB_{NF} =115%)

Fig. S3 Comparison of observed and simulated (BASE and NF) daily surface solar radiation for Beijing and Tianjin in January 2013.

3.2 PBL height

The observations on PBL height are not available, so the NCEP FNL reanalysis PBL height are used to evaluate PBL predictions. The original NCEP FNL ($1^o \times 1^o$) are linearly interpolated into 36 and 12 km grid resolutions, as shown in the first column of Fig. S4. The simulated PBL height in BASE and NF, as well as their differences in absolute value and percentage over Domain 1 and Domain 2 are presented in Fig. S4. It can be seen that the simulated PBL heights, of both BASE and NF, are consistent to the assimilated PBL over both Domain 1 and 2. The overall statistics are summarized in Table S5. In general, the average predicted PBL height of BASE over Domain 1 are lower than that of NF (524.7 m vs. 514.9 m), as well as over Domain 2 (332.1 m vs. 318.5 m), indicating that the direct aerosol feedbacks will result in an decrease in PBL height of about 1.9% on average over Domain 1 and 4.3% over Domain 2. Although the predicated PBL height of NF over Domain 1 is more close to the reanalysis data (526.2 m), the RMSE, NME, and Corr. Coeff. of BASE are slightly better than the NF predictions. After nested into Domain 2, all the performance statistics of BASE are better than those of NF. The BASE scenario slightly under estimates the PBL height (by -6.6 m, -2.0%) but NF overestimates by 7.0 m, 2.2%.

Table S5. Overall statistics of PBL predictions of the BASE and NF over Domain 1 and 2.

Simulation name	Grid size /(km)	Reanalysis /(m)	Sim. /(m)	MB /(m)	RMSE /(m)	NMB /(%)	NME /(%)	Corr. Coeff.
BASE	36	526.2	514.9	-11.4	138.3	-2.2	17.3	0.932
NF			524.7	-1.6	141.8	-0.3	18.3	0.928
BASE	12	325.1	318.5	-6.6	97.0	-2.0	20.8	0.843
NF			332.1	7.0	99.0	2.2	22.5	0.834

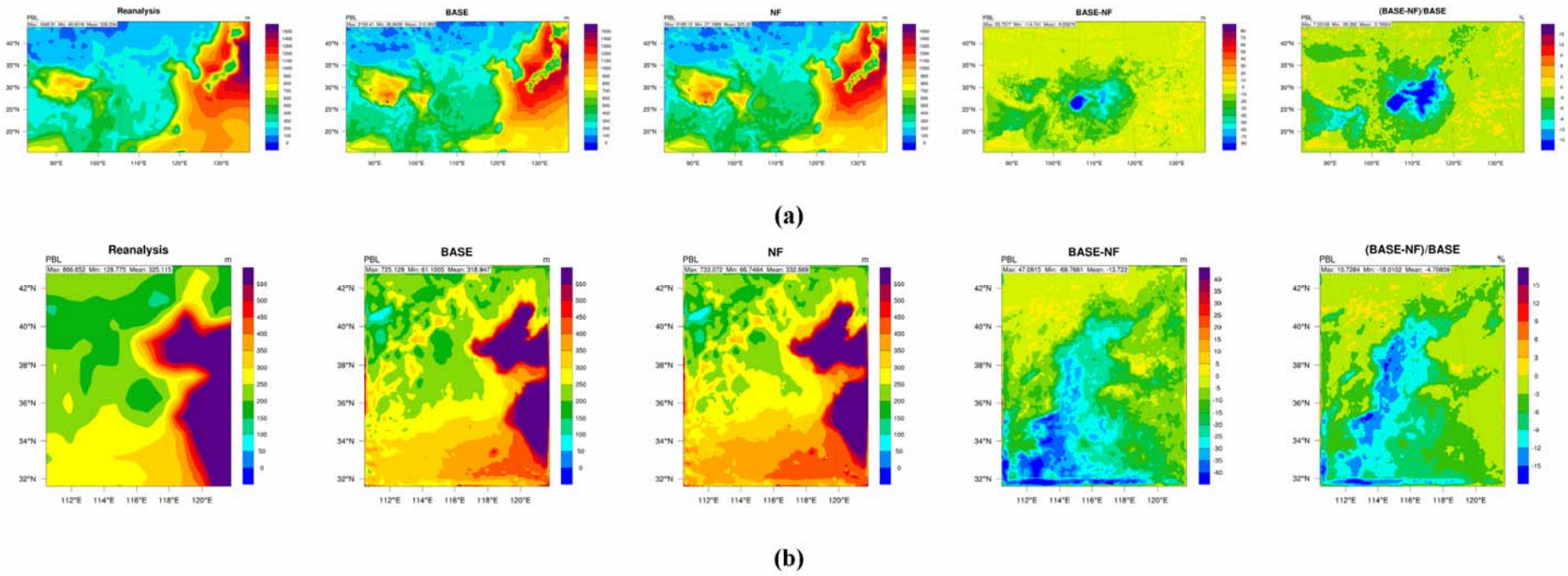

Fig. S4. NCEP FNL assimilated and simulated PBL height in the BASE and NF simulations, and their differences in absolute value (BASE-NF) and percentage ((BASE-NF)/BASE) over Domain 1 (a) and Domain 2 (b).

As shown in the comparison of BASE and NF in Fig. S4, the most significant decrease occurs over the areas in the central eastern China (Fig. S4a), which is similar to the reductions in SWDOWN, at a level about 20–90 m (4–18%). When nested into Domain 2 (Fig. S4b), the decrease in PBL height is more obvious in the southern area of Hebei, where the three top polluted cities locate, and central and eastern area of Henan, at a level of 20–50 m (4–18%). In Wang et al. [26], the decrease in PBL in Beijing due to feedbacks is estimated as 14.5%, which is also consistent to this study.

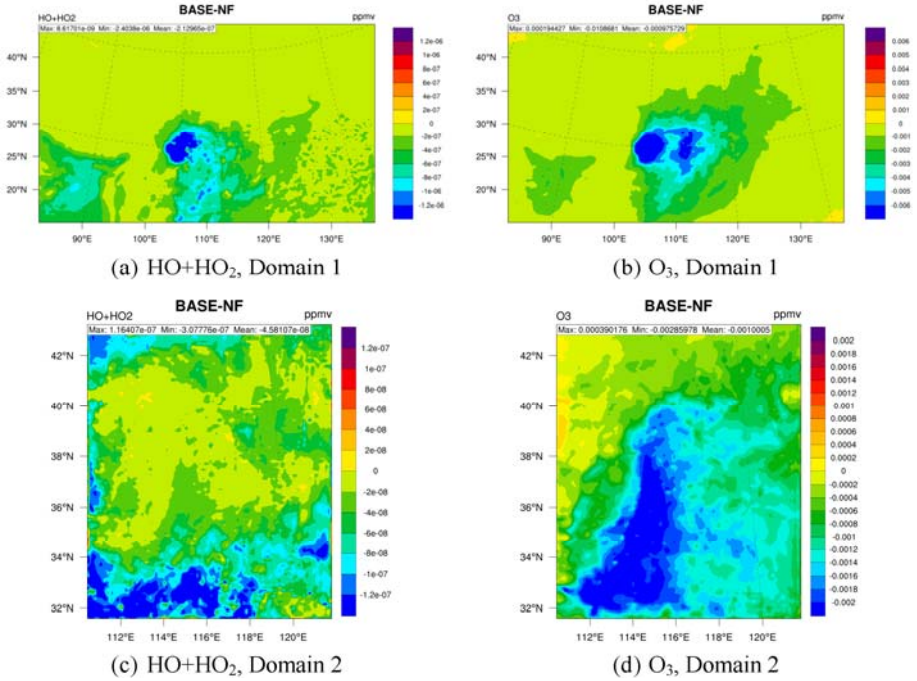

Fig. S5. Aerosol direct effects (BASE-NF) on the concentrations of free radicals ($HO+HO_2$) and O_3 over Domain 1 (a and b) and Domain 2 (c and d).

4 Comparison with other studies

Table S6 presents the comparison between this study and the other previous studies mentioned in the introduction. It can be seen that our results are consistent with those studies in terms of the influences of the aerosol feedbacks on SWDOWN, PBL height, and $PM_{2.5}$ concentrations. It also can be seen that extended simulations with longer period and different seasons may need to be considered in future studies.

Table S6. Comparison of this study with other previous studies.

Studies	Gao et al. [39]	Wang et al. [26]	Gao et al. [28]	Zhang et al. [27]	This study
Model	WRF/Chem 3.5.1	WRF 3.4/CMAQ 5.0	WRF/Chem 3.3	WRF/Chem 3.3	WRF/Chem 3.6.1
Simulation period	January, 2010	January, 2013	January 2–26, 2013	January, 2013	January, 2013
Domain	East Asia (81-km), northern China (27-km), northern Hebei (9-km)	East Asia (36-km)	East China (27-km)	East China (27-km)	East Asia (36-km), northern China (12-km)
Horizontal resolution	81-, 27-, and 9-km	36-km	27-km	27-km	36- and 12-km
Vertical resolution	27 layers to 100 mb	23 layers to 100 mb	51 layers to 50 mb	28 layers to 50 mb	23 layers to 100 mb
Anthropogenic	MEIC 2010	Zhao et al. [40]	MEIC 2010	MEIC 2010	MEIC 2010

emissions					
Gas-phase chemistry	CBMZ	CB05	CBMZ	CBMZ	CBMZ
Aerosol module	MOSAIC 8 bin	AERO6	MOSAIC 8 bin	MOSAIC 4 bin	MOSAIC 8 bin
SWDOWN	-30–80% in Beijing	-26% in Beijing, -31% in Tianjin	-8–36 $W \cdot m^{-2}$	Up to -84 $W \cdot m^{-2}$	-20–34 $W \cdot m^{-2}$ (16%–30%) in southern Hebei on monthly ave.
PBL	-278.2 m in Shijiazhuang	-140 m (20%) in Beijing	-22–207m (8–32 %)	Up to -268 m	-20–50 m (4%–18%) in southern Hebei on monthly ave.
$PM_{2.5}$ concentration	+20 $\mu g \cdot m^{-3}$ in Shijiazhuang	+20% in Beijing, +15% in Shijiazhuang, 12% in Tianjin, 15% in Jinan	+10–50 $\mu g \cdot m^{-3}$ over NCP	Up to +17.8 $\mu g \cdot m^{-3}$ in Sichuan Basin	+3–9% over southern Hebei on monthly ave., up to 50 $\mu g \cdot m^{-3}$ when $PM_{2.5} > 400$ $\mu g \cdot m^{-3}$

References

1. Li M, Zhang Q, Streets D G, He K B, Zhang Y. Mapping Asian anthropogenic emissions of non-methane volatile organic compounds to multiple chemical mechanisms. Atmospheric Chemistry and Physics, 2014, 14: 5617–5638
2. Guenther A, Karl T, Harley P, Wiedinmyer C, Palmer P I, Geron C. Estimates of global terrestrial isoprene emissions using MEGAN (Model of Emissions of Gases and Aerosols from Nature). Atmospheric Chemistry and Physics, 2006, 6: 3181–3210
3. Shaw W J, Allwine K J, Fritz B G, Rutz F C, Rishel J P, Chapman E G. An evaluation of the wind erosion module in DUSTRAN. Atmospheric Environment, 2008, 42: 1907–1921
4. Gong S L, Barrie L A, Blanchet J P. Modeling sea-salt aerosols in the atmosphere: 1. Model development. Journal of Geophysical Research, 1997, 102: 3805–3818
5. Gong S L, Barrie L A, Propspero J M, Savoie D L, Ayers G P, Blanchet J P, Spacek L. Modeling sea-salt aerosols in the atmosphere: 2. Atmospheric concentrations and fluxes. Journal of Geophysical Research, 1997, 102: 3819–3830
6. Gong S L. A parameterization of seasalt aerosol source function for sub and supermicron particles. Global Biogeochemical Cycles, 2003, 17(4): 1097
7. Zaveri R A, Peters L K. A new lumped structure photochemical mechanism for largescale applications. Journal of Geophysical Research, 1999, 104: 30387–30415
8. Zaveri R A, Easter R C, Fast J D, Peters L K. Model for simulating aerosol interactions and chemistry (MOSAIC). Journal of Geophysical Research, 2008, 113: D13204
9. Madronich S, Fl℃ke S. The role of solar radiation in atmospheric chemistry. In: Boule P, eds. Handbook of Environmental Chemistry. Heidelberg: Springer_Verlag, 1993, 126
10. Ikeda R, Kusaka H. Proposing the simplification of the multilayer urban canopy model: intercomparison study of four models. Journal of Appllied Meteorology and Climatology, 2010, 49: 902–919
11. Chou M D, Suarez M J, Ho C H, Yan M H, Lee K T. Parameterizations for cloud overlapping and shortwave single scattering properties for use in general circulation and cloud ensemble models. Journal of Climate, 1998, 11: 202–214
12. Mlawer E J, Taubman S J, Brown P D, Iacono M J, Clough S A. Radiative transfer for inhomogeneous atmospheres: RRTM, a validated Parameterizations for cloud overlapping and shortwave single scattering properties for use in general circulation and cloud ensemble models correlated k model for the longwave. Journal of Geophysical Research, 1997, 102(D14): 16663–16682
13. Ek M B, Mitchell K B, Lin Y, Rogers B, Grunmann P, Koren V, Gayno G, Tarpley J D. Implementation of NOAH land surface model advances in the National Centers for Environmental Prediction operational mesoscale Eta model. Journal of Geophysical Research, 2003, 108(D22): 8851
14. Janjić Z I. Nonsingular Implementation of the Mellor–Yamada Level 2.5 Scheme in the NCEP Meso Model. NCEP Off. Note 437, 61. Camp Springs: National Center for Environmental Prediction, 2001.
15. Hong S Y, Noh Y, Dudhia J. A new vertical diffusion package with an explicit treatment of entrainment processes. Monthly Weather Review, 2006, 134: 2318–2341
16. Grell G A, Devenyi D. A generalized approach to parameterizing convection combining ensemble and data assimilation techniques. Geophysical Research Letters, 2002, 29(14): 1693
17. Chen S H, Sun W Y. A one dimensional time dependent cloud model. Journal of the Meteorological S℃iety of Japan, 2002, 80: 99–118
18. Zhang Y, Wen X Y, Jang C. Simulating chemistry-aerosol-cloud-radiation-climate feedbacks over the continental U.S. using the online-coupled Weather Research Forecasting Model with chemistry (WRF/Chem). Atmospheric Environment, 2010, 44: 3568–3582
19. Wang L T, Zhang Y, Wang K, Zheng B, Zhang Q, Wei W. Application of Weather Research and Forecasting Model with Chemistry (WRF/Chem) over northern China: Sensitivity study, comparative evaluation, and policy implications. Atmospheric Environment, 2016, 124: 337–350
20. Grell G A, Peckham S E, Schmitz R, McKeen S A, Frost G, Skamarock W C, Eder B. Fully coupled “online” chemistry within the WRF model. Atmospheric Environment, 2005, 39: 6957–6975
21. Zhang Y, B℃quet M, Mallet V, Seigneur C, Baklanov A. Real-time air quality forecasting, part I: History,

techniques, and current status. Atmospheric Environment, 2012, 60: 632–655
22. Zhang Y, Chen Y S, Sarwar G, Schere K. Impact of gas-phase mechanisms on Weather Research Forecasting Model with Chemistry (WRF/Chem) predictions: Mechanism implementation and comparative evaluation. Journal of Geophysical Research, 2012, 117: D01301
23. Emery C, Tai E, Yarwood G. Enhanced Meteorological Modeling and Performance Evaluation for Two Texas Ozone Episodes. Final Report. Houston: The Texas Natural Resource Conservation Commission, 2001. Available online at http://www.tceq.state.tx.us/assets/public/implementation/air/am/contracts/reports/mm/EnhancedMetModelingAndPerformanceEvaluation.pdf.
24. Tesche T W, McNally D E, Emery C A, Tai E. Evaluation of the MM5 Model Over the Midwestern U.S. for Three 8-hour Oxidant Episodes. Wright: Alpine Geophysics, LLC and Novato: ENVIRON International Corp., 2001
25. Wang L T, Wei Z, Yang J, Zhang Y, Zhang F F, Su J, Meng C C, Zhang Q. The 2013 severe haze over southern Hebei, China: model evaluation, source apportionment, and policy implications. Atmospheric Chemistry and Physics, 2014, 14: 3151–3173
26. Wang J D, Wang S X, Jiang J K, Ding A J, Zheng M, Zhao B, Wong D C, Zhou W, Zheng G J, Wang L, Pleim J E, Hao J M. Impact of aerosol–meteorology interactions on fine particle pollution during China's severe haze episode in January 2013. Environmental Research Letters, 2014, 9: 094002
27. Zhang B, Wang Y X, Hao J M. Simulating aerosol–radiation–cloud feedbacks on meteorology and air quality over eastern China under severe haze conditions in winter. Atmospheric Chemistry and Physics, 2015, 15: 2387–2404
28. Gao Y, Zhang M, Liu Z, Wang L, Wang P, Xia X G, Tao M. Modeling the feedback between aerosol and meteorological variables in the atmospheric boundary layer during a severe fog–haze event over the North China Plain. Atmospheric Chemistry and Physics, 2015, 15: 4279–4295
29. Carter W P L. A Detailed Mechanism for the Gas-Phase Atmospheric Reactions of Organic Compounds. Atmospheric Environment, 1990, 24: 481–518
30. Carter W P L. Implementation of the SAPRC99 chemical mechanism into the Models-3 Framework. Report to the U.S. EPA. Riverside: Statewide Air Pollution Research Center, University of California, 2000
31. Shrivastava M, Fast J, Easter R, Gustafson J W I, Zaveri R A, Jimenez J L, Saide P, Hodzic A. Modeling organic aerosols in a megacity: comparison of simple and complex representations of the volatility basis set approach. Atmospheric Chemistry and Physics, 2011, 11: 6639–6662
32. Kain J S. The Kain Fritsch convective parameterization: An update. Journal of Applied Meteorology, 2004, 43: 170–181
33. Ginoux P, Chin M, Tegen I, Prospero J, Holben B, Dubovik O, Lin S J. Sources and global distributions of dust aerosols simulated with the G℃ART model. Journal of Geophysical Research, 2001, 106: 20255–20273
34. U.S. EPA. Guidance on the Use of Models and Other Analyses for Demonstrating Attainment of Air Quality Goals for Ozone, $PM_{2.5}$, and Regional Haze. Research Triangle Park: Office of Air and Radiation/Office of Air Quality Planning and Standards, 2007
35. Boylan J W, Russell A G. PM and light extinction model performance metrics, goals, and criteria for three-dimensional air quality models. Atmospheric Environment, 2006, 40: 4946–4959
36. Wei Z, Wang L T, Chen M Z, Zheng Y. The 2013 severe haze over the Southern Hebei, China: $PM_{2.5}$ composition and source apportionment. Atmospheric Pollution Research, 2014, 5: 759-768
37. Wang Y X, Zhang Q Q, Jiang J K, Zhou W, Wang B Y, He K B, Duan F K, Zhang Q, Philip S, Xie Y Y. Enhanced sulfate formation during China's severe winter haze episode in January 2013 missing from current models. Journal of Geophysical Research: Atmospheres, 2014, 119: 10425–10440
38. Zheng B, Zhang Q, Zhang Y, He K B, Wang K, Zheng G J, Duan F K, Ma Y L, Kimoto T. Heterogeneous chemistry: a mechanism missing in current models to explain secondary inorganic aerosol formation during the January 2013 haze episode in North China. Atmospheric Chemistry and Physics, 2015, 15: 2031–2049
39. Gao M, Carmichael G R, Wang Y S, Saide P E, Yu M, Xin J Y, Liu Z, Wang Z F. Modeling study of the 2010 regional haze event in the North China Plain. Atmospheric Chemistry and Physics, 2016, 16: 1673–1691
40. Zhao B, Wang S X, Dong X Y, Wang J D, Duan L, Fu X, Hao J M, Fu J. Environmental effects of the recent emission changes in China: implications for particulate matter pollution and soil acidification. Environmental Research Letters, 2013, 8: 024031